Noise filtering for accurate measurement of line edge roughness and critical dimension from SEM images

Dehua Li, Rui Guo, Soo-Young Lee, Jin Choi, Seom-Beom Kim, Sung-Hoon Park, In-Kyun Shin, and Chan-Uk Jeon

Citation: Journal of Vacuum Science & Technology B **34**, 06K604 (2016); doi: 10.1116/1.4968184
View online: http://dx.doi.org/10.1116/1.4968184
View Table of Contents: http://scitation.aip.org/content/avs/journal/jvstb/34/6?ver=pdfcov
Published by the AVS: Science & Technology of Materials, Interfaces, and Processing

Articles you may be interested in

Practical approach to modeling e-beam lithographic process from SEM images for minimization of line edge roughness and critical dimension error
J. Vac. Sci. Technol. B **34**, 011601 (2016); 10.1116/1.4937740

An atomic force microscopy-based method for line edge roughness measurement
J. Appl. Phys. **113**, 104903 (2013); 10.1063/1.4794368

Understanding the relationship between true and measured resist feature critical dimension and line edge roughness using a detailed scanning electron microscopy simulator
J. Vac. Sci. Technol. B **28**, C6H34 (2010); 10.1116/1.3517717

Measuring line roughness through aerial image contrast variation using coherent extreme ultraviolet spatial filtering techniquesa)
J. Vac. Sci. Technol. B **23**, 2844 (2005); 10.1116/1.2134717

Correlation of atomic force microscopy sidewall roughness measurements with scanning electron microscopy line-edge roughness measurements on chemically amplified resists exposed by x-ray lithography
J. Vac. Sci. Technol. B **17**, 2723 (1999); 10.1116/1.591053

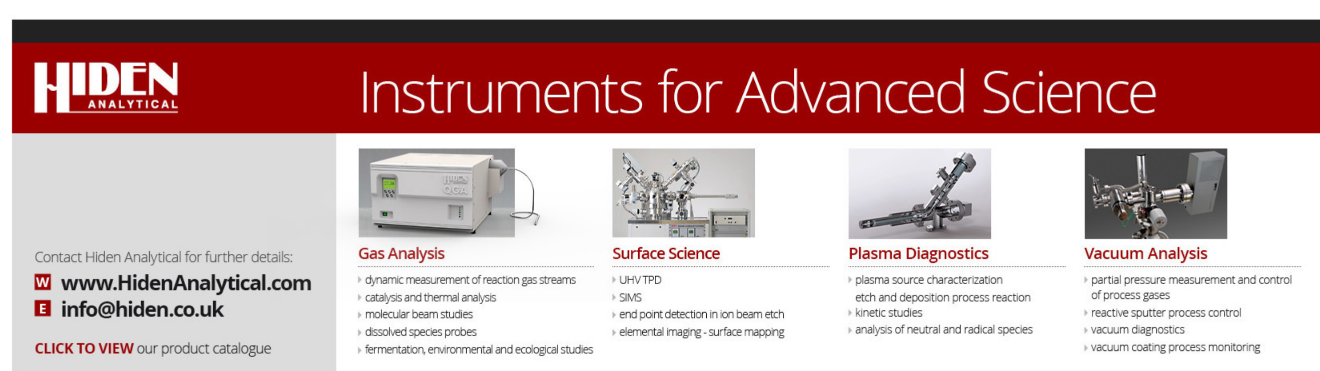

Redistribution subject to AVS license or copyright; see http://scitation.aip.org/termsconditions. IP: 131.204.21.179 On: Mon, 12 Dec 2016 21:57:01

Noise filtering for accurate measurement of line edge roughness and critical dimension from SEM images

Dehua Li, Rui Guo, and Soo-Young Lee[a)]
Department of Electrical and Computer Engineering, Auburn University, Auburn, Alabama 36849

Jin Choi, Seom-Beom Kim, Sung-Hoon Park, In-Kyun Shin, and Chan-Uk Jeon
Samsung Electronics, Mask Development Team, 16 Banwol-Dong, Hwasung, Kyunggi-Do 445-701, South Korea

(Received 1 July 2016; accepted 8 November 2016; published 21 November 2016)

Measurements of the line edge roughness (LER) and critical dimension (CD) from scanning electron microscope (SEM) images are often required for analyzing circuit patterns transferred onto substrate systems. A common approach is to employ image processing techniques to detect feature boundaries from which the LER and CD are computed. SEM images usually contain a significant level of noise which affects the accuracy of measured LER and CD. This requires reducing the noise level by a certain type of low-pass filter before detecting feature boundaries. However, a low-pass filter also tends to destroy the boundary detail. Therefore, a careful selection of low-pass filter is necessary in order to achieve the high accuracy of LER and CD measurements. In this paper, a practical method to design a Gaussian filter for reducing the noise level in SEM images is proposed. The method utilizes the information extracted from a given SEM image in adaptively determining the sharpness and size of a Gaussian filter. The results from analyzing the effectiveness of the Gaussian filter designed by the proposed method are provided. © *2016 American Vacuum Society*.
[http://dx.doi.org/10.1116/1.4968184]

I. INTRODUCTION

Circuit patterns are transferred onto the resist layer by various lithographic processes including electron beam (e-beam) lithography.[1–5] The fidelity of transferred patterns is often examined through scanning electron microscope (SEM) imaging.[6,7] Feature boundaries in SEM images are determined, from which metrics such as critical dimension (CD) and line edge roughness (LER) are computed. As the feature size continues to decrease, it has become even more important to be able to measure the CD and LER accurately from SEM images.[8,9] A small error in determining feature boundaries can lead to a significant deviation of the CD and LER from the actual values.

A typical approach to determining feature boundaries in a SEM image is to employ image processing techniques such as edge detection or modeling. What makes the image processing nontrivial is the noise contained in SEM images. A standard procedure is to apply a noise-reduction filter, e.g., low-pass filter, to SEM images before further processing. It is common that the noise level is significant and varies with SEM image. Also, the type of noise may be different for a different image or a different location within an image. Therefore, it is not optimal to use a fixed filter in general. In this study, the issue of designing a noise-reduction filter, taking the characteristics of noise into account, is addressed.

There are several types of noise-reduction filters widely used in image processing. The median filter is known to be effective in removing pixels corrupted by the "salt-and-pepper" noise (shot noise), but not as effective for spatially correlated noise. It tends to destroy fine details, e.g., thin lines, line ends, etc., and only the filter size can be controlled. Another filter often used is the spatial-averaging filter which reduces the noise level while it is not able to remove each individual noise pixel completely. A side-effect of applying the averaging filter is that the image contrast is lowered, blurring the feature boundaries. However, a more sophisticated control in designing a filter is possible through weighted averaging. In the previous work,[10,11] a fixed filter was employed to reduce the noise level in processing SEM images. Therefore, the image-dependent noise characteristics such as the noise level were not considered. In this paper, a practical method for designing a Gaussian filter adaptively based on the noise characteristics of each SEM image is described. In the method, the noise characteristics are extracted from the frequency-domain representation of SEM image, and the sharpness (standard deviation) and size of Gaussian filter are determined based on a certain measure derived from the characteristics.

One of the methods to detect feature boundaries with or without noise filtering is to rely on edge modeling, i.e., fitting the brightness distribution over a feature boundary to a model function. The effectiveness of this approach was well demonstrated using the Gaussian function as a model function through an elaborated investigation.[12] Nevertheless, it is worthwhile to point out the sensitivity of the method to the shape of brightness distribution. When the bright distribution has a significantly different shape from the model function, this can lead to a substantial error in the detected feature boundaries. Also, in their study, it appears that only the "simple noise" was considered in the accuracy analysis. Another method for the boundary detection following a noise reduction step is to employ an edge detector which is normally a differential operator. This method is more

[a)]Electronic mail: leesooy@eng.auburn.edu

Redistribution subject to AVS license or copyright; see http://scitation.aip.org/termsconditions. IP: 131.204.21.179 On: Mon, 12 Dec 2016 21:57:01

flexible from the viewpoint of applicability and is computationally less expensive, though it requires a careful determination of edge pixels. In this study, an edge detector is used in analyzing the effectiveness of the Gaussian filter designed by the proposed filter-design method. A spatially correlated noise is considered in this analysis for more realistic results.

The rest of the paper is organized as follows. The issue of processing SEM images is addressed in Sec. II. The proposed method of filter design is described in Sec. III and the edge detection in Sec. IV. The results are discussed in Sec. V, followed by a summary in Sec. VI.

II. NOISE FILTERING

SEM images inherently contain a significant level of noise as shown Fig. 1. Therefore, it is unavoidable to reduce the noise level before any image processing technique for detecting feature boundaries can be applied. The noise filtering greatly affects the accuracy of detected feature boundaries. That is, an inappropriate level of noise filtering can cause a significant error in the measured LER and CD as illustrated in Fig. 2 where a simulated SEM image with the known LER and CD is employed. An under-filtering leads to a rougher detected boundary than the actual one such that the measured LER, for example, is 31% larger than the actual LER [see Fig. 2(a)]. On the other hand, an over-filtering makes the detected boundary smoother than the actual, leading to a negative error (−24%) in the measured LER [see Fig. 2(b)].

A two-dimensional (2D) Gaussian filter is selected for noise filtering in this study, for its applicability and controllability. The level of noise filtering can be adjusted by controlling the sharpness and size of a Gaussian filter. In the 2D Gaussian function given in Eq. (1) and illustrated in Fig. 3, the sharpness is determined by the standard deviation σ. The larger the σ is, the higher level of noise filtering is achieved, i.e., the noise is filtered more, but more blurring occurs. On the other hand, for a smaller σ, the noise is filtered less. Given a σ, the filter size W (see Fig. 3) determines the domain over which the filtering is carried out for each pixel. A larger W tends to reduce the noise level more, but also blur the image more

$$g(x,y) = \frac{1}{2\pi\sigma^2} e^{-(x^2+y^2)/(2\sigma^2)}. \tag{1}$$

The objective of the proposed method for designing the Gaussian filter is to determine the filter parameters, σ and W, which minimize the differences between the measured and actual LER's and CD's. The determination of the two parameters is guided by the characteristics of a given SEM image, in particular, the signal and noise characteristics.

III. FILTER DESIGN

The objective of noise filtering is to reduce the noise as much as possible while keeping the signal (feature boundaries) as much as possible. However, in general, reducing the noise also reduces the signal, and therefore, the level of noise filtering must be properly selected such that the accuracy of boundary detection is sufficiently high. In the case of a Gaussian filter, the level of noise filtering can be controlled by the two parameters of filter, σ and W. In particular, the proposed design method determines σ and W using a metric which quantifies the relative signal level after filtering. For evaluating the metric, the frequency-domain representations of signal and noise are employed. However, the signal and noise are not readily separable in an image. Therefore, given a SEM image, they are estimated in the frequency domain.

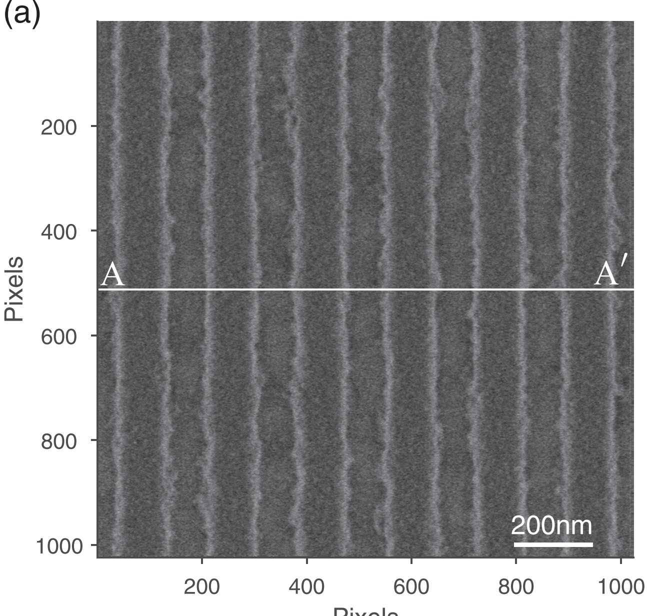

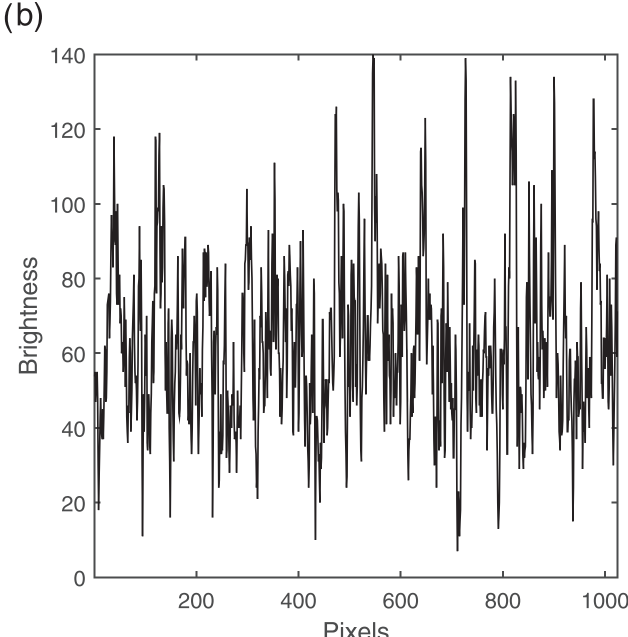

Fig. 1. (a) Example of SEM image of a L/S pattern and (b) brightness distribution along the line A-A′ of in the SEM image in (a).

Let $i(x, y)$ represent the brightness distribution in a SEM image of size $M \times M$. The frequency-domain representation, $I(u, v)$, is obtained through the 2D discrete Fourier transform (just "Fourier transform" hereafter) as in

Redistribution subject to AVS license or copyright; see http://scitation.aip.org/termsconditions. IP: 131.204.21.179 On: Mon, 12 Dec 2016 21:57:01

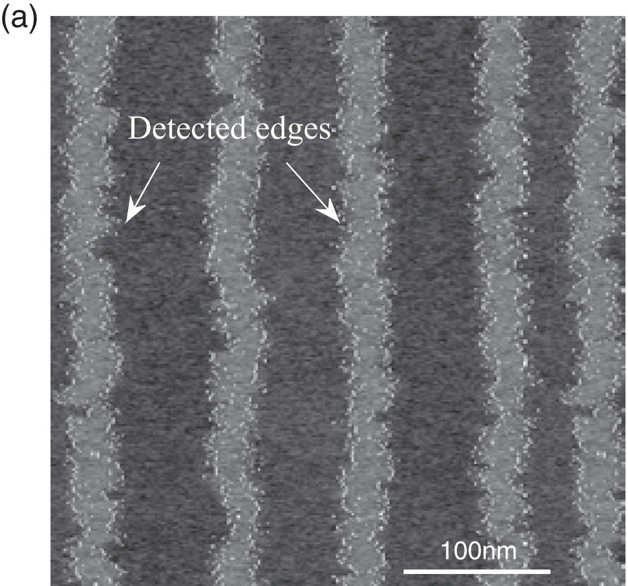

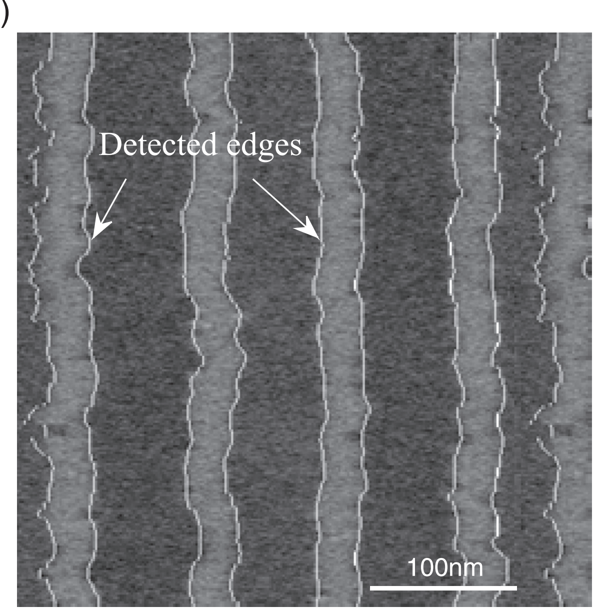

FIG. 2. Edge detection results following (a) under-filtering and (b) over-filtering of noise.

$$I(u,v) = \sum_{x=0}^{M-1}\sum_{y=0}^{M-1} i(x,y)e^{-j(2\pi(ux+vy)/M)}. \quad (2)$$

A SEM image and the corresponding Fourier transform are shown in Fig. 4. The $|I(u,v)|$ shows different behaviors along the u and v dimensions. This is due to the fact that lines are vertically oriented and the noise is more spatially correlated in the x direction than in the y direction. It should be noted that $I(u, v)$ includes both the signal and noise.

In order to estimate the noise, "flat regions" (i.e., excluding boundary regions) are extracted from the SEM image, to generate an image of "sampled" noise, as shown in Fig. 5(a). The sampled noise contains the noise and DC biases where the DC biases come from the different brightness levels of the inside and outside of a feature. The DC bias is removed from each flat region to leave only the noise. The sampled noise consisting of the extracted flat regions is smaller than the corresponding SEM image at least in one dimension, $m \times M$ in the case of a L/S pattern, where $m < M$ [see Fig. 5(a)]. The zero-padding is done to the sampled noise to make its size $M \times M$. The sampled noise after the DC removal and zero-padding is denoted by $n(x, y)$.

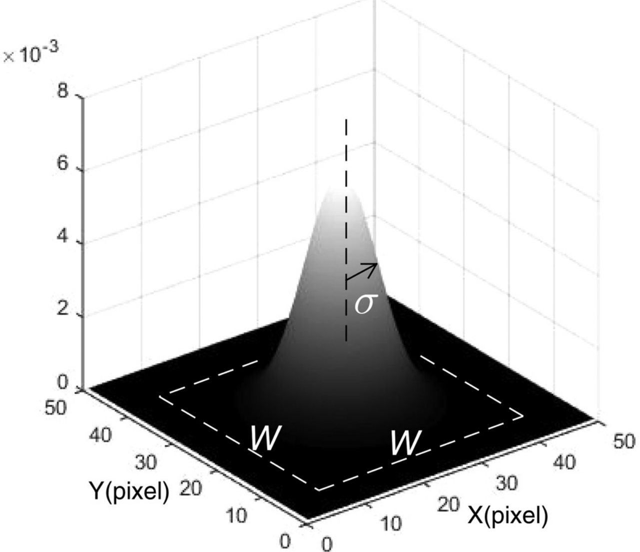

FIG. 3. Two-dimensional Gaussian filter of size $W \times W$ with the standard deviation of σ.

The frequency-domain representation of $n(x, y)$ can be obtained through the Fourier transform. However, due to the fact that the size of sampled noise before the zero-padding is smaller than that of the SEM image, a scaling on the Fourier transform results to make it comparable to $I(u, v)$. Let $N(u, v)$ denote the scaled Fourier transform of $n(x, y)$, which can be expressed as

$$N(u,v) = \sqrt{\frac{M}{m}}\sum_{x=0}^{M-1}\sum_{y=0}^{M-1} n(x,y)e^{-j\left(2\pi(ux+vy)/M\right)}. \quad (3)$$

In Fig. 5(b), the plot of $|N(u,v)|$ is provided. It is seen that $|N(u,v)|$ does not vary with v while it does significantly with u. As pointed out earlier, this is due to the larger spatial correlation of noise in the x direction, which is related to the scanning direction of electron beam, contributing to the higher amplitudes of low frequency components. This may suggest the use of an anisotropic filter. However, in this study, the isotropic (radially symmetric) Gaussian filter is adopted (1) for the simplicity, (2) since a pattern may include both vertical and horizontal boundaries of features, and (3) the scanning direction can be in either direction.

The Fourier transform of a Gaussian function is also of Gaussian in the frequency domain. Let us denote the Fourier transform by $G(u, v)$ which may be expressed as in

$$G(u,v) = \frac{1}{2\pi\sigma_f^2}e^{-(u^2+v^2)/(2\sigma_f^2)}, \quad (4)$$

Redistribution subject to AVS license or copyright; see http://scitation.aip.org/termsconditions. IP: 131.204.21.179 On: Mon, 12 Dec 2016 21:57:01

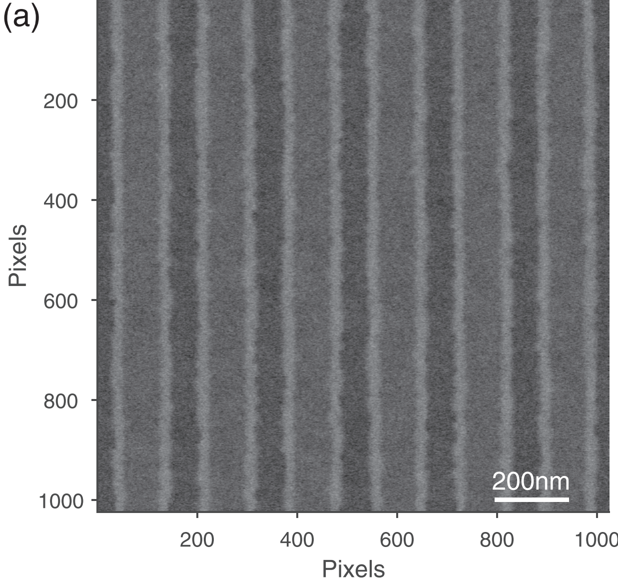

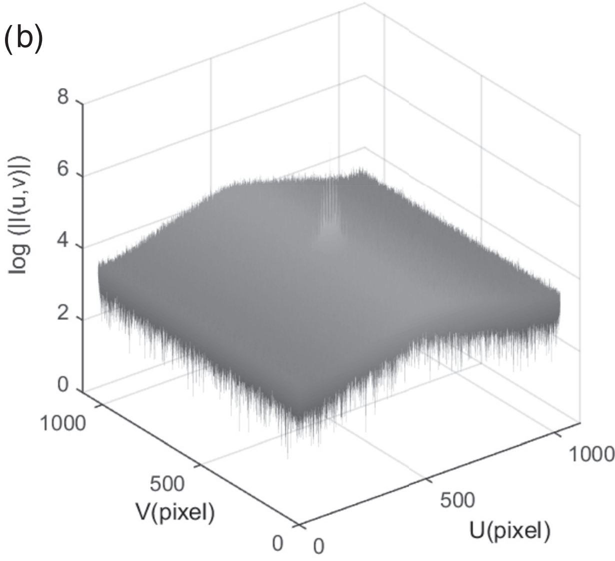

FIG. 4. (a) SEM image $i(x, y)$ of size 1024×1024 and (b) the frequency-domain representation $|I(u, v)|$ plotted in the logarithmic scale.

where σ_f is the standard deviation of $G(u, v)$ in the frequency domain, to be referred to as *cut-off frequency*.

The proposed method for designing a Gaussian filter determines the cut-off frequency σ_f from which the spatial-domain Gaussian filter can be derived. Let us define *total image intensity* to be $\sum_{u=0}^{M-1}\sum_{v=0}^{M-1}|I(u,v)|G(u,v)$, which is the sum of all frequency components in a SEM image filtered by the Gaussian filter. Similarly, *total noise intensity* is defined as $\sum_{u=0}^{M-1}\sum_{v=0}^{M-1}|N(u,v)|G(u,v)$, which is the sum of all frequency components in the sampled noise filtered by the Gaussian filter. Then, the *total signal intensity* may be approximated to be $\sum_{u=0}^{M-1}\sum_{v=0}^{M-1}|I(u,v)|G(u,v) - \sum_{u=0}^{M-1}\sum_{v=0}^{M-1}|N(u,v)|G(u,v)$.

In Fig. 6, the total signal intensity and total noise intensity are plotted as functions of σ_f for a typical SEM image. When

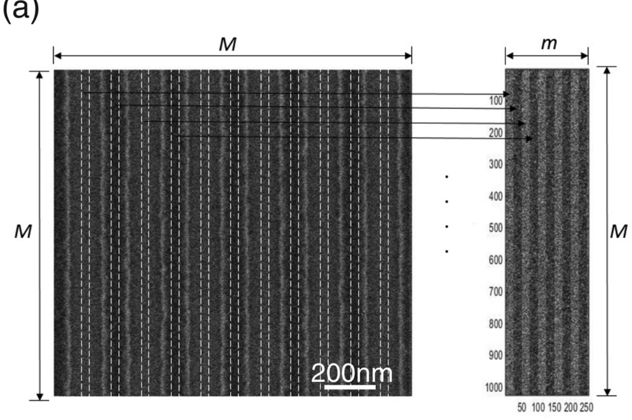

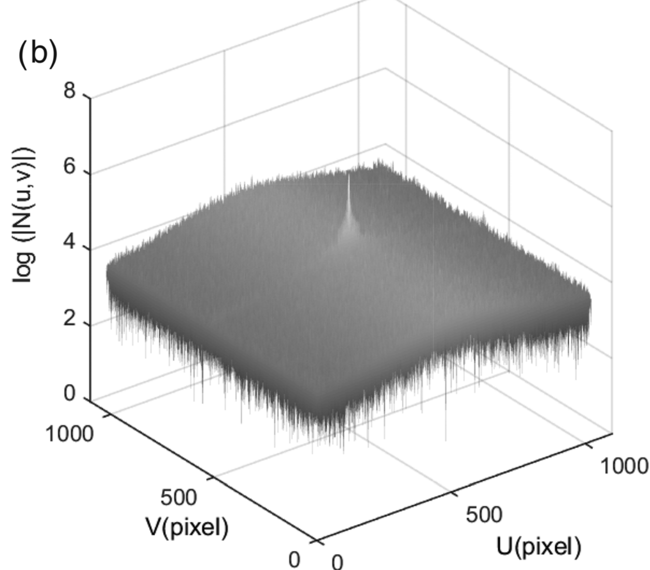

FIG. 5. (a) Generation of sampled noise $n(x, y)$ (before the DC is removed) and (b) the frequency-domain representation $|N(u, v)|$ in the logarithmic scale.

the cut-off frequency σ_f is very small (approaching to a zero), the total signal intensity is greater than the total noise intensity unless the noise is dominant. As σ_f increases, both the total signal intensity and total noise intensity monotonically decrease since $G(u, v)$ is a normalized Gaussian. But, the total signal intensity decreases faster since the signal is normally band-limited. Therefore, the total signal and noise intensities intersect at a certain σ_f. In the proposed method, σ_f at which the signal-to-noise ratio defined in Eq. (5) becomes 1 is used in designing the Gaussian filter. The rationale behind this selection of the cut-off frequency is to reduce the noise level as much as possible under the condition that the signal level is not less than the noise level

$$\text{signal-to-noise ratio} = \frac{\sum_{u=0}^{M-1}\sum_{v=0}^{M-1}|I(u,v)|G(u,v) - \sum_{u=0}^{M-1}\sum_{v=0}^{M-1}|N(u,v)|G(u,v)}{\sum_{u=0}^{M-1}\sum_{v=0}^{M-1}|N(u,v)|G(u,v)}. \tag{5}$$

Redistribution subject to AVS license or copyright; see http://scitation.aip.org/termsconditions. IP: 131.204.21.179 On: Mon, 12 Dec 2016 21:57:01

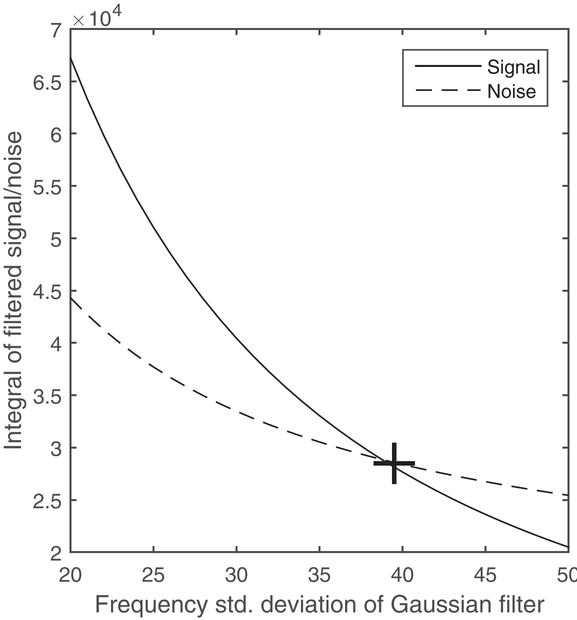

FIG. 6. Total signal and noise intensities as functions of the cut-off frequency σ_f of the Gaussian filter. In designing the Gaussian filter, σ_f at which the two intensities become equal (marked by "+") is used.

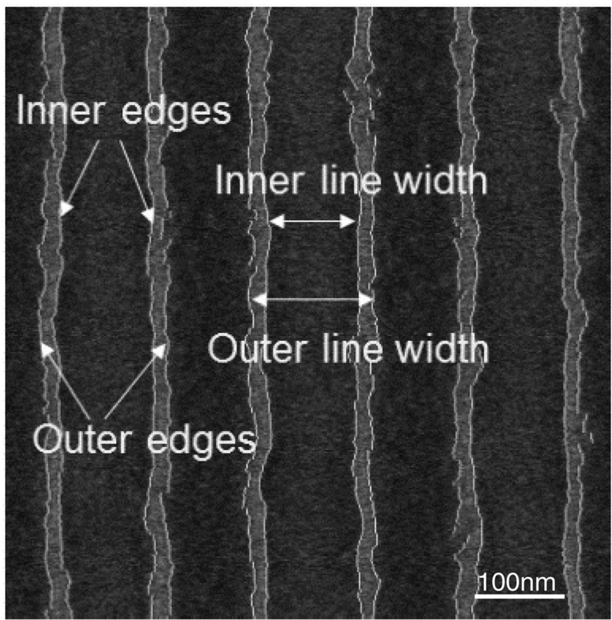

FIG. 7. Each boundary of a feature (line) is characterized by a bright band, and both edges of the band region are detected resulting in inner and outer edges.

In the continuous case, the Fourier transform of $e^{-t^2/(2\sigma^2)}$ is given as $\sqrt{2\sigma^2\pi}e^{-2\sigma^2(\pi f)^2}$. That is, the standard deviation in the spatial domain, σ, is related to the standard deviation in the frequency domain, σ_f, as $2\pi\sigma\sigma_f = 1$. But, in the discrete case, the relationship becomes $2\pi\sigma\sigma_f = M$, where M is the size of an image. Therefore, the standard deviation of Gaussian filter in the spatial domain can be derived from the cut-off frequency as in

$$\sigma = \frac{M}{2\pi\sigma_f}. \quad (6)$$

The size of Gaussian filter, W, is determined such that most of the significant portion of Gaussian function is included. In this study, W is set to 6σ (note that the distance from the filter center of to the filter boundary is 3σ). At 3σ, a Gaussian function decreases to 1.11% of the peak value

$$W = 6\sigma. \quad (7)$$

A digital filter is normally symmetric, and therefore, 6σ is rounded up to the closest odd integer. It should be clear that the Gaussian filter specified by σ and W adapts itself to each individual SEM image according to the signal and noise levels in the image.

IV. DETECTION OF FEATURE BOUNDARIES

In the remaining resist profile, the boundary of a feature is defined by a surrounding sidewall which is brighter than other regions in the (secondary-electron) SEM image (see Fig. 7). A band of white region appears along the feature boundary, and both sides of the band, i.e., *inner* and *outer* boundaries, are detected in this study. These boundaries are where the spatial change of image brightness is largest.[13] That is, the gradient of image brightness is either locally maximum or minimum at the boundaries (see Fig. 8). In the case of a L/S pattern, starting from the outside of a line, the first four maximum and minimum gradients correspond to outer, inner, inner, and outer edges (boundaries), respectively (refer to Fig. 7).

The designed Gaussian filter is applied to SEM images to reduce the noise level. Then, feature boundaries are detected by finding the local maximum and minimum of brightness gradient in the filtered image. A standard edge detector such

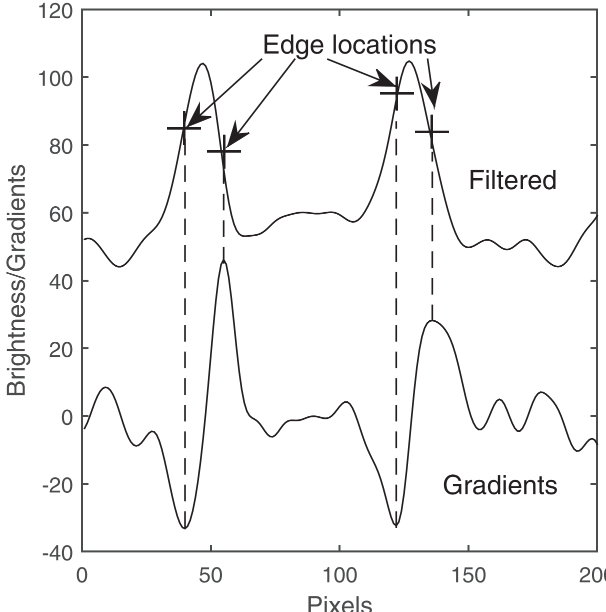

FIG. 8. Maximum and minimum brightness gradients correspond to (inner and outer) edge locations.

Redistribution subject to AVS license or copyright; see http://scitation.aip.org/termsconditions. IP: 131.204.21.179 On: Mon, 12 Dec 2016 21:57:01

as Sobel operator can be employed to compute the gradient of the brightness distribution. The Sobel operator for vertical boundaries (as in the SEM images in this paper) is

$$\begin{bmatrix} -1 & 0 & 1 \\ -2 & 0 & 2 \\ -1 & 0 & 1 \end{bmatrix}.$$

The search of the maximum and minimum gradients is carried out row-by-row (for vertical lines). In order to guide the searching, an edge region is defined around each peak in the filtered SEM image, as shown in Fig. 9. Then, the maximum and minimum gradients are searched within edge regions.

Though detecting the inner and outer boundaries (edges) is considered in this study, one may want to find the boundary where the brightness is highest, i.e., peaks (see Fig. 9). The brightness peaks, which are normally between the inner and outer boundaries, may be searched within edge regions following the noise filtering (without computing the brightness gradient). Or, the peak detection can be done readily by locating the zero-crossings in the brightness gradient (refer to Fig. 8). Note that the brightness peak is where the brightness gradient changes its sign, from negative to positive or positive to negative.

V. RESULTS AND DISCUSSION

For analyzing the effectiveness of a Gaussian filter designed by the proposed method, "reference (SEM) images" are generated from real SEM images. Feature boundaries in each reference image and therefore the LER and CD are known. To reference images, a spatially correlated noise rather than a simple noise such as shot (salt-and-pepper) noise is added to test the filter for realistic cases. The noise level in each reference image is varied for a thorough analysis. One of the four reference images used in this study is shown in Fig. 10, and the known CDs and LERs for the reference images are provided in Table I. After the noise filtering and boundary detection, the inner and outer line

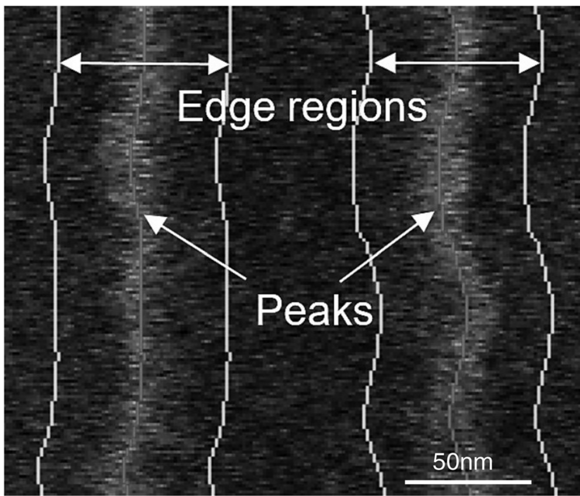

FIG. 9. Edge regions are defined around peaks and the maximum and minimum gradients are found within edge regions.

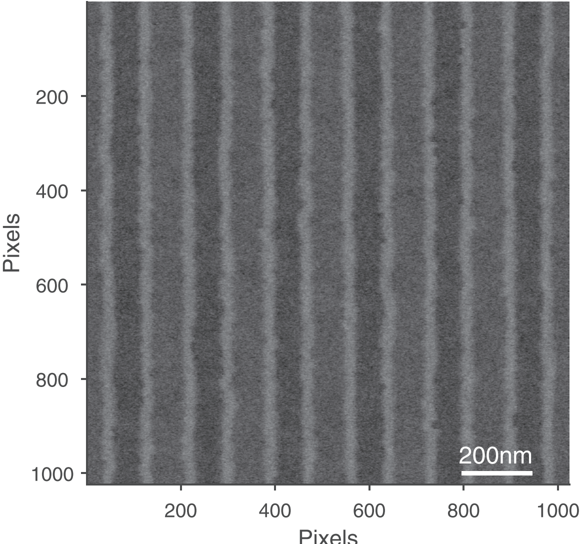

FIG. 10. Example of reference SEM image where the same noise level as in the corresponding original SEM image is added.

widths are measured from the detected inner and outer edges, respectively (refer to Fig. 7). Then, the CD is computed as the average of the inner and outer line widths, and the LER is quantified as the standard deviation of edge location, i.e., $1-\sigma$ LER, considering both inner and outer edges. The accuracy of measurement, i.e., detecting feature boundaries using the Gaussian filter designed by the proposed method is analyzed using the CD and LER deviations defined in Eqs. (8) and (9)

$$\text{LER Dev} = \frac{\text{LER}_m - \text{LER}_k}{\text{LER}_k} \times 100\%, \quad (8)$$

$$\text{CD Dev} = \frac{\text{CD}_m - \text{CD}_k}{\text{CD}_k} \times 100\%, \quad (9)$$

where LER_m and LER_k are the measured and known LER's, respectively, and CD_m and CD_k the measured and known CD's, respectively.

In each reference image, four difference noise levels are considered in order to test the adaptability of the Gaussian filter designed by the proposed method. The σ and W of the designed Gaussian filter, LER and CD measured, and percent LER and CD deviations for each noise level are provided for the four reference images in Tables II–V.

First, it can be seen from the tables that the Gaussian filter designed by the proposed method is effective in reducing the

TABLE I. Known LER and CD in the four reference images generated from SEM images obtained with four different doses where the target line width is 120 nm.

Reference image	LER (nm)	CD (nm)
Ref. image 1	5.51	116.38
Ref. image 2	3.42	128.15
Ref. image 3	2.93	133.74
Ref. image 4	2.71	144.50

Redistribution subject to AVS license or copyright; see http://scitation.aip.org/termsconditions. IP: 131.204.21.179 On: Mon, 12 Dec 2016 21:57:01

TABLE II. CD and LER measured from the reference image 1, and the deviations from the known CD and LER, are provided with the noise level varied from 13.2 to 27.9 dB. The filter parameters (W and σ) are also included in each case.

	Ref. image 1					
SNR (dB)	W (nm)	σ (nm)	LER (nm)	CD (nm)	LER Dev (%)	CD Dev (%)
13.2	35.25	5.60	5.59	116.26	1.51	−0.11
16.0	26.79	4.03	5.76	116.33	4.61	−0.05
20.0	18.33	2.64	5.81	116.33	5.57	−0.04
27.9	9.87	1.21	5.60	116.41	1.73	0.02

TABLE III. CD and LER measured from the reference image 2, and the deviations from the known CD and LER, are provided with the noise level varied from 13.2 to 28.0 dB. The filter parameters (W and σ) are also included in each case.

	Ref. image 2					
SNR (dB)	W (nm)	σ (nm)	LER (nm)	CD (nm)	LER Dev (%)	CD Dev (%)
13.2	46.53	7.41	3.38	128.11	−1.29	−0.03
16.0	32.43	5.34	3.55	128.17	3.71	0.02
20.1	21.15	3.48	3.70	128.11	8.27	−0.03
28.0	9.87	1.64	3.59	128.16	4.95	0.01

TABLE IV. CD and LER measured from the reference image 3, and the deviations from the known CD and LER, are provided with the noise level varied from 13.8 to 28.5 dB. The filter parameters (W and σ) are also included in each case.

	Ref. image 3					
SNR (dB)	W (nm)	σ (nm)	LER (nm)	CD (nm)	LER Dev (%)	CD Dev (%)
13.8	46.53	7.41	2.89	133.66	−1.32	−0.06
16.5	32.43	5.34	3.07	133.74	4.95	0.00
20.6	21.15	3.48	3.19	133.77	8.86	0.02
28.5	9.87	1.64	3.09	133.76	5.67	0.01

TABLE V. CD and LER measured from the reference image 4, and the deviations from the known CD and LER, are provided with the noise level varied from 14.3 to 28.8 dB. The filter parameters (W and σ) are also included in each case.

	Ref. image 4					
SNR (dB)	W (nm)	σ (nm)	LER (nm)	CD (nm)	LER Dev (%)	CD Dev (%)
14.3	43.71	7.18	2.70	144.32	−0.38	−0.12
17.0	32.43	5.22	2.83	144.52	4.45	0.02
21.1	21.15	3.43	2.93	144.52	7.95	0.02
28.8	12.69	1.68	2.86	144.45	5.34	−0.03

noise level and achieving the high accuracy in the measured LER and CD in all cases. Specifically, the average LER deviation is 4.4%, and the maximum LER deviation is 8.86%. The CD deviation is less than 1% in all cases. The reason for the extremely small CD deviation is that the error in the detected edge location is not directly reflected in the CD deviation (note that the CD depends on both left and right edges) and the CD is averaged along the length dimension of feature (line). Second, one important observation is that the high accuracy is achieved independent of the noise level. This well demonstrates the good adaptability of the design method. As the SNR increases (i.e., the noise level decreases), the σ decreases since the noise needs to be filtered less. Third, the LER deviation tends to be smaller for a higher level of noise in some of the reference images and is negative in some of the highest levels of noise. This might be due to the slight over-filtering by the Gaussian filter, making the detected boundaries smoother.

It is worthwhile to point out that the LER deviation is caused by both the noise and filtering. The noise tends to make the measured LER increase. On the other hand, the filtering does the opposite by reducing the high frequency components of LER. Depending on which effect is more dominant, one may get an over-estimation or underestimation of LER.

The proposed method is also applied to four real SEM images from which the reference images are generated. These SEM images were obtained by using four different dose levels for a L/S pattern (L = S = 120 nm). A real SEM image is shown along with the detected boundaries in Fig. 11. The Gaussian filter designed, and CD and LER measured are provided in Table VI. It is not possible to quantify the accuracy of the detected boundaries in these images since the actual CD and LER are not known. However, it appears by visual inspection that the detected boundaries are accurate. As the dose level increases, the measured CD becomes larger as expected. Also, the measured LER is smaller for a higher dose level. This is consistent with the well-known behavior of LER. A higher dose leads to a smaller relative stochastic fluctuation of exposure (energy deposited in the resist), which makes the LER smaller.

The overall procedure including the filter design, boundary detection, and computation of CD and LER is computationally efficient. It takes only a few seconds for a SEM image of size 1024 × 1024 with 12 lines (24 edges per row) on a PC (Intel Xeon, 3.4 GHz, 8-G RAM). It is worthwhile to point out that the computational requirement of an edge modeling approach is much higher since each edge needs to be modeled individually through a time-consuming error-minimization procedure.

VI. SUMMARY

In this paper, a practical method to design a Gaussian filter which plays a critical role in achieving a high accuracy of detecting feature boundaries in SEM images is described. Given a SEM image, the proposed method utilizes the frequency-domain representations of the signal and noise

Redistribution subject to AVS license or copyright; see http://scitation.aip.org/termsconditions. IP: 131.204.21.179 On: Mon, 12 Dec 2016 21:57:01

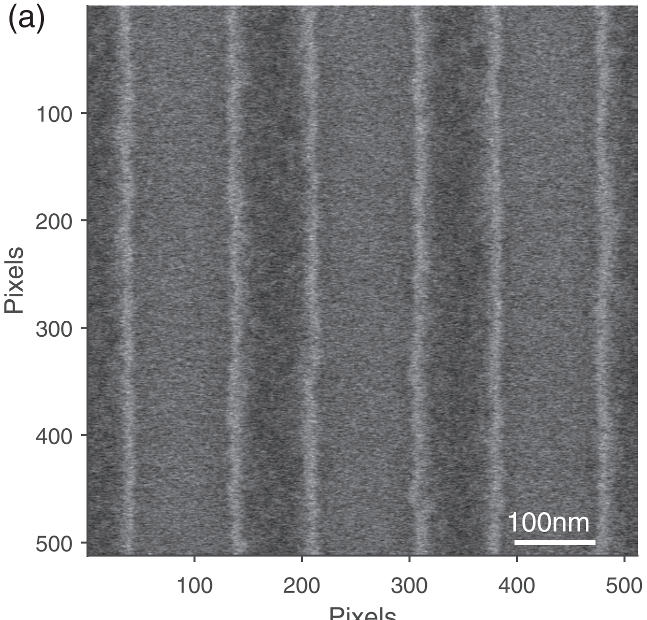

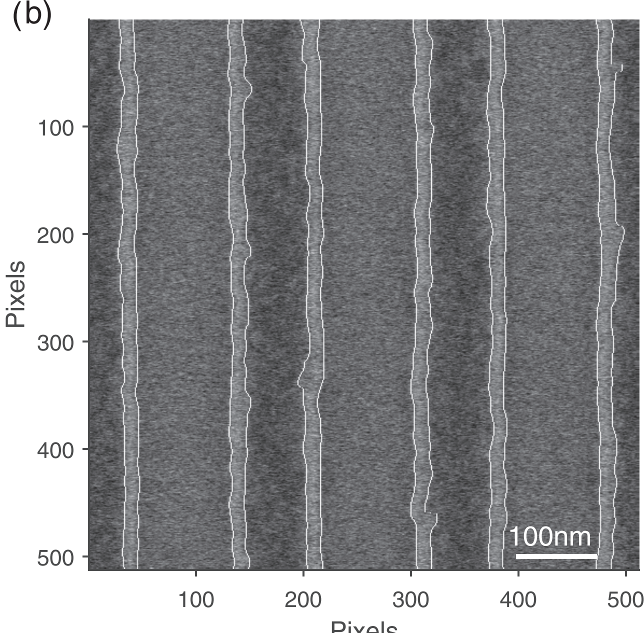

FIG. 11. (a) Example of real SEM image and (b) feature boundaries detected in SEM image in (a).

estimated from the image in order to determine the shape (standard deviation) and size of Gaussian filter. This allows to adaptively determine the level of filtering depending on the relative noise level. Using a set of reference images for which the LER and CD are known, the effectiveness of the Gaussian filter designed by the proposed method has been verified. In all cases considered, a high accuracy is achieved with the average LER deviation less than 5% and the average CD deviation less than 1%. It is worthwhile to point out that the high accuracy is achieved for various noise levels, which well demonstrates the good adaptability.

The proposed method is able to design an effective filter without requiring a complicated design procedure and is computationally efficient. Therefore, it is believed that the proposed design method has a good potential to be a useful tool.

TABLE VI. Filter parameters, and measured CD and LER for the SEM images obtained with different normalized doses, 0.705, 0.774, 0.845, and 1.082.

	Original images			
Dose[a]	W (nm)	σ (nm)	LER (nm)	CD (nm)
0.705	43.71	6.97	4.66	115.16
0.774	40.89	6.57	3.12	125.42
0.845	40.89	6.75	2.70	132.09
1.082	43.71	7.42	2.24	144.14

[a]Normalized dose.

ACKNOWLEDGMENT

This work was supported by a research grant from Samsung Electronics Co., Ltd.

[1]A. A. Tseng, K. Chen, C. D. Chen, and K. J. Ma, IEEE. Trans. Electron. Packag. Manuf. **26**, 141 (2003).
[2]R. Murali, D. Brown, K. Martin, and J. Meindl, J. Vac. Sci. Technol., B **24**, 2936 (2006).
[3]M. J. Burek and J. R. Greer, Nano. Lett. **10**, 69 (2010).
[4]Q. Dai, S.-Y. Lee, S.-H. Lee, B.-G. Kim, and H.-K. Cho, Microelectron. Eng. **88**, 902 (2011).
[5]W. Chen and H. Ahmed, Appl. Phys. Lett. **62**, 1499 (1993).
[6]M. Okada and S. Matsui, Jpn. J. Appl. Phys., Part 1 **54**, 118004 (2015).
[7]S. Babin, K. Bay, and J. J. Hwu, J. Vac. Sci. Technol., B **28**, C6H1 (2010).
[8]A. Yamaguchi, R. Tsuchiya, H. Fukuda, O. Komuro, H. Kawada, and T. Iizumi, Proc. SPIE **5038**, 689 (2003).
[9]M. Yoshizawa and S. Moriya, J. Vac. Sci. Technol., B **20**, 1342 (2002).
[10]G. P. Patsis, V. Constantoudis, A. Tserepi, E. Gogolides, and G. Grozev, J. Vac. Sci. Technol., B **21**, 1008 (2003).
[11]R. Guo, S.-Y. Lee, J. Choi, S.-H. Park, I.-K. Shin, and C.-U. Jeon, J. Vac. Sci. Technol., B **34**, 011601 (2016).
[12]T. Verduin, P. Kruit, and C. W. Hagen, J. Micro/Nanolithogr. MEMS MOEMS **13**, 033009 (2014).
[13]M. A. Sutton, N. Li, D. C. Joy, A. P. Reynolds, and X. Li, Exp. Mech. **47**, 775 (2007).

Redistribution subject to AVS license or copyright; see http://scitation.aip.org/termsconditions. IP: 131.204.21.179 On: Mon, 12 Dec 2016 21:57:01